Proceedings of the
Annual Stability Conference
Structural Stability Research Council
Atlanta, Georgia, April 21-24, 2020

Strength of cold formed sections subjected to axial compressive force and bending moments

M.T.Hanna[1], Mohamed Massoud[2], E.A.Amoush[3]

Abstract
Cold formed sections are usually made of thin plates that make them susceptible to fail in three basic modes which are local, distortional, and global. Moreover, due to the redistribution of stresses after sectional (local/distortional) buckling they can carry additional loads up to failure. These additional capacities depend on the interaction of the plate slenderness ratios and the overall member slenderness ratios. Consequently, they are behaving differently than sections that do not exhibit sectional (local/distortional) buckling modes. Therefore, the objective of this paper is to make an in-depth investigation for the capacity of steel cold formed section columns subjected to axial compressive force in-addition to either major or minor axis bending moments. For this purpose, a nonlinear finite element model has been constructed using the commercial software, ANSYS. Thin-shell elements with four nodes and six degrees of freedom at each node were used to model the columns. Both large deflection analysis and elasto-plastic material response have been incorporated in the model. Newton-Raphson iterations were used in solving the nonlinear system of equations. Pin-ended support conditions with overall geometric imperfections of l/1000 are adopted in this study. Both lipped channel and sigma sections are considered. Further, a group of sections varied in their thickness are selected. In-addition, wide range of column slenderness are examined to explore the transition between the different modes of failure (local, distortional, and global). Results reflect that for the two studied sections, the axial-bending interaction diagrams are not linear, and concave upward, providing significant additional capacity to that predicted by the linear interaction equation that is adopted in the North American specification, AISI-2017.

1. Introduction

Cold formed steel members are widely used in steel construction market. They are characterized by high strength weight ratio, environmental friendly, and durability. CFS can easily be bent into

[1] Professor, Housing and Building National Research Center, Egypt <m_tawfick2003@yahoo.com>
[2] Professor, Housing and Building National Research Center, Egypt<m_massoud2002@yahoo.com>
[3] Associate Professor, Higher Technological Institute,Egypt <essamamoush2008@yahoo.com>

various shapes which have obvious design advantages. The most common of these shapes are channels, lipped channels, sigma sections, Z sections, and hat sections. The sigma shaped section has recently used as an alternative to the channel section as a stud in the wall bearing system.

Cold formed sections often fail in three basic modes which are local, distortional, and global. Local and distortional modes are characterized by entire deformations, whether translation or bending, of the plates forming the section, while global buckling represents the whole motion in the cross section. Nandini and Kalyanaraman (2010) studied the interaction of local, distortional and lateral torsional buckling by a finite element method for a thin-walled cold-formed lipped channel. Their results show that the nonlinear finite element method can be used to study the interaction of different buckling modes. Hong-Guang Luo, et.al., (2011) presented a procedure to obtain the distortional critical stress of cold-formed channel beams with inclined simple edge stiffeners, bent about the minor axis. They showed that the flexural deformation of the flange is not negligible. Li and Chen (2008) presented an analytical model for predicting the critical stress of distortional buckling of compression flange and lip in channel, zed and sigma sections under either compression or bending about an axis perpendicular to the web.

Generally, thin plates can carry additional loads after buckling had happened due to the redistribution of stresses. This additional capacity depends on several factors such as; the width-thickness ratios of the plates forming the sections, degree of freedom at the ends of the plates (the intersection lines of the plates forming the sections), and the state of stresses within them. Therefore, local and distortional buckling modes have certain post buckling reserve capacities, however, global buckling has insignificant amount. There has been considerable research on the behavior and strength of thin walled sections. A.H.Salem, et. al (2007) found that strength of the slender I-sections members depends on the flange and web width-thickness ratios as well as member slenderness ratios. Inaddition, Interaction curves between axial loads and major axis bending moments are almost linear for the different member slenderness ratios. D.J.Klingshirn, et al., (2010) tested fifty-eight sigma shaped specimens subjected to concentrated axial compression at various lengths to generate local, distortion, and global buckling failure modes. They tested specimens with or without holes, and concluded that, AISI design methods, effective width and DSM, are good predictors of ultimate strength of sigma sections. Silvestre and Camotim (2004), used the generalized beam theory, GBT, to drive analytical formulae for the critical buckling lengths and bifurcation stress in cold-formed steel C and Z-section members subjected to pure bending with arbitrary sloping single-lip stiffeners and end support conditions. Schafer B.W., (2008) focused primarily on the use of the semi-analytical finite strip method and collapse modeling using shell finite elements. He compared between the finite strip and finite element solutions and the importance of imperfections, residual stresses, boundary conditions, element choice, element discretization, and solution controls in the collapse modeling of cold-formed steel sections. Shahabeddin Torabian, et. al (2014, 2015) predict the structural strength of cold-formed steel lipped channels under combined axial force and biaxial bending moments. Results are compared to both current, and a newly proposed Direct Strength Method (DSM) for beam-columns. The new method provides capacity predictions on average 20% higher than current design formulations. In addition they tested short length Z-section under several combination of biaxial bending moments and axial compressive force. They found that the cross-sectional applied stress distribution is the most important parameter in modulating the failure mechanisms, such as local or distortional buckling. In addition, the member ductility is strongly correlated to the degree of eccentricity in the axial load.

The objective of the paper is to compare the structural response of lipped channel as well as sigma cold formed sections under combination of axial force and major as well as minor axis bending moments. The major and minor axis bending moments will be acted separately.

2. Parametric Study Variables

Lipped channel as well as sigma sections are chosen for the study. The total web depth for the channel and sigma was 250mm. However, for the sigma section the web is divided into different parts as shown in Fig. 1-a. For both sections the flange width and lip depth was 60mm, and 20mm; respectively. Two thicknesses were examined which are 1.5mm, and 2.5mm. For each cross section, two member slenderness ratios, L/r_y = 50 & 150, are chosen to study the different modes of failure (local, distortional, and overall). The basic cases that consists of members having hinges at both ends and bend about major as well as minor axis in single curvature as shown in Fig.1-b were studied in this paper.

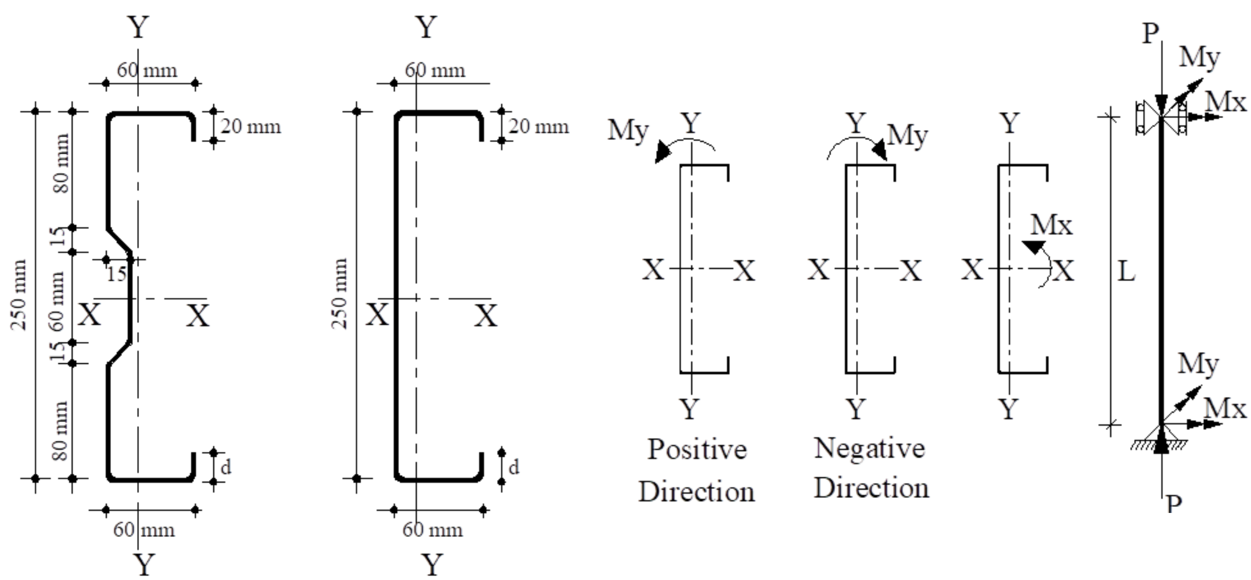

a) Cross section studied b) Cases of loading and boundary condition

Figure 1: Case of Study

3 - Finite Element Model

A three-dimensional nonlinear finite element model is developed in the present study using ANSYS finite element package (2012). Thin-shell elements with four nodes and six degrees of freedom per node are used to model the channel and sigma columns as shown in Fig. 2. Modeling of the cross sections rounded corners are treated as flat junction. The elastic modulus of elasticity and yield stress of the steel material were considered as 210,000 MPa and 240 MPa; respectively. The shear modulus was taken equal to 81,000 MPa. Both large deflection analysis and bilinear elasto-plastic material model obeying von Mises yield criterion was adopted. The boundary conditions for beam-column elastic line were treated as pinned at both ends. However, thick plates (t= 10mm) are added at the supports to ensure the stress distribution and maintain the geometry of column end cross sections. These plates will relatively prevent warping deformations at these ends. Hinged supports are simulated as follows, the four nodes at the corners along with the node that represent the center of gravity at both end sections are prevented from translations along the horizontal X and Y directions. However, the center of gravity point at one end is prevented from translation along the vertical Z-axis, while at the other end where axial concentrated load is applied, is allowed to move along Z-axis. These boundary conditions permit the rotation of the end sections around X and Y axis, Fig.2-a. Axial loads as well as major and minor axis bending moments are applied at the center of gravity point. Axial concentrated load is applied at one end, while the bending moments are applied at the both ends, in directions that cause single curvature of the column, Fig. 2-b. The loads are applied on the members sequentially. The axial force is applied first from zero to a certain value, this value is kept constant, and then the bending moments are increased from zero to the ultimate value. Time curves of the axial load and the end bending moments are shown in Fig.2-c. Load control technique is used to control the increment of the external loads. Newton–Raphson iterations were used in solving the nonlinear system of equations.

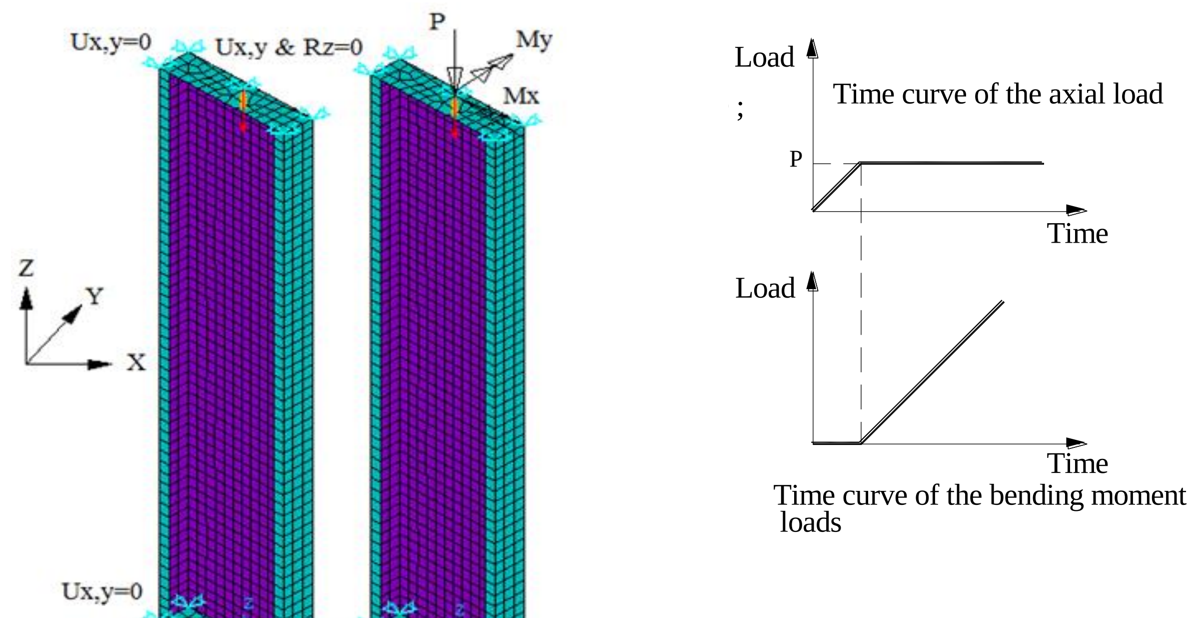

c) Time curves of different load applied

a) Boundary conditions b) Loads applied

Figure 2: Nonlinear finite element model

The numerical model is verified against the experimental results in El Aghoury et al., (2017) where they tested eight single sigma section columns under axial loads. They measured the geometric imperfections as well as the residual stresses in the specimens. V. M. Zeinoddini and B. W. Schafer, (2012) introduced three methods to simulate imperfection fields. Further, they investigated material and geometric nonlinear finite element collapse modeling to simulate the strength and behavior of the cold-formed steel members by using the effect of these different approaches. They concluded that the 1D model approach is the most accurate approach for predicting the strength, axial flexibility, and failure mechanism of those members.

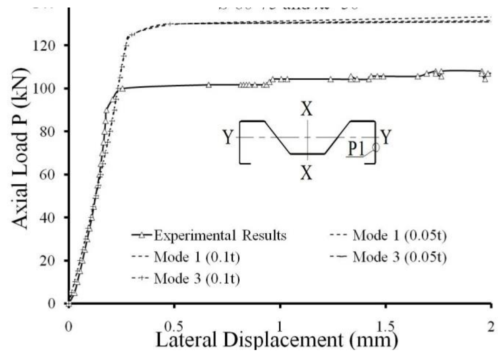

a) Sectional imperfections

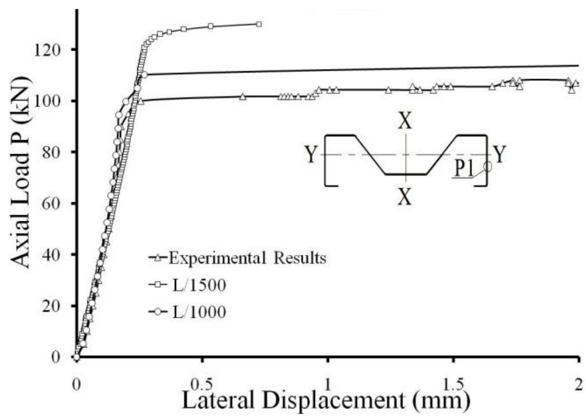

b) overall geometric imperfections

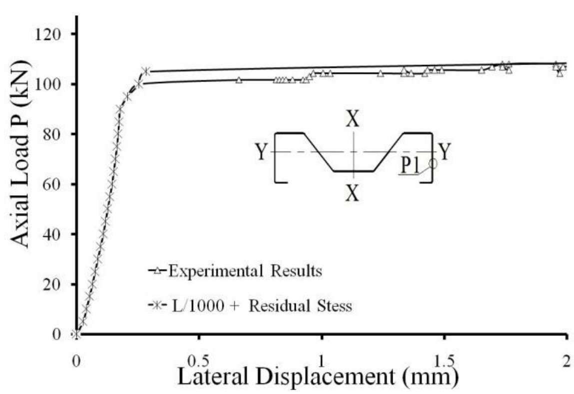

c) Residual and overall geometric imperfections

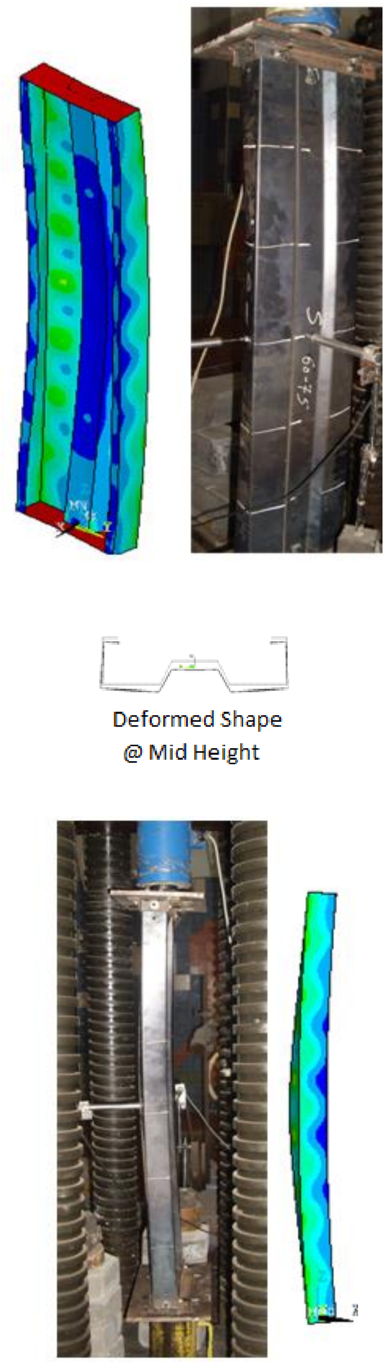

d) Experimental and numerical failure mode

Figure. 3. Comparison between experimental, El Aghoury, et. al. (2017), and the developed finite element model.

In this study, the sectional geometric imperfections are considered in the finite element model by assuming the elastic buckling mode 1 and mode 3 with imperfection values equal to 0.05t, and 0.1t. However, the overall geometric imperfections have been modeled by assuming the column bent about the minor axis "Y" in a half sine wave in the direction that causes compression in the lips. The measured average membrane residual stress pattern by El Aghoury, et. al. (2017) is applied in the model as a pre-stress, which is kept constant while the externally applied load increases up gradually to the failure load. Comparison are plotted in Fig. 3 for specimen S-60-75. It is depicted that, the experimental and numerical ultimate load as well as the failure shapes are comparable. In addition, the sectional imperfections have no remarkable effect on the ultimate axial capacity of the columns. However, the axial capacity decreased by 12% when the overall imperfection values increase from L/1500 to L/1000. Moreover, when the residual stress pattern is added to the overall imperfection of L/1000, the axial capacity decreased further by an average 4%.

4 - Interaction Diagrams

4-1 Axial compressive force and major axis bending moment

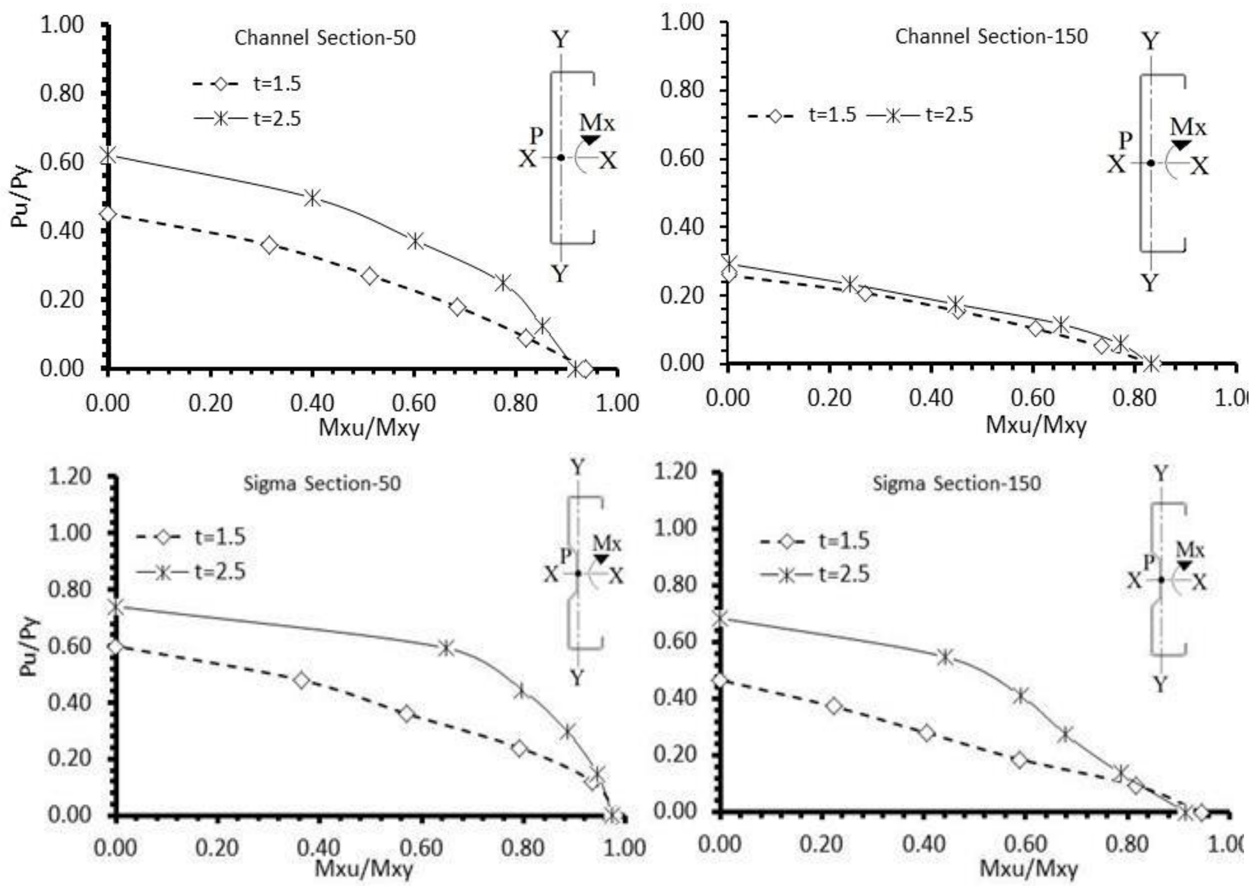

$L/r_y = 50$ $L/r_y = 150$

Figure. 4 Relation between Pu/Py and Mxu/Mxy

The developed finite element model is used in the extended parametric study. The value of the overall geometric imperfections is set equal to L/1000, where L is the total length of the column. As mentioned before, the sectional (local/distortional) geometric imperfections have no remarkable effect on the ultimate loads, therefore, these type of imperfections are not considered. Also, for simplicity the effect of residual stresses is ignored.

The ultimate axial compressive force, P_u are normalized with respect to the squash load, P_y (P_y = A x F_y), also the ultimate major axis bending moments, M_{xu}, are normalized with respect to the first yield major axis bending moments, M_{xy} (M_{xy} = S_x x F_y). Where S_x and A are the elastic modulus and the area of the full section; respectively. The interaction curves between, P_u/P_y and M_{xu}/M_{xy} are drawn in Fig. 4 for the channel and sigma sections. Strength of sections with different thicknesses as well as member slenderness ratios are plotted on the figure.

t = 1.5mm

t = 2.5mm

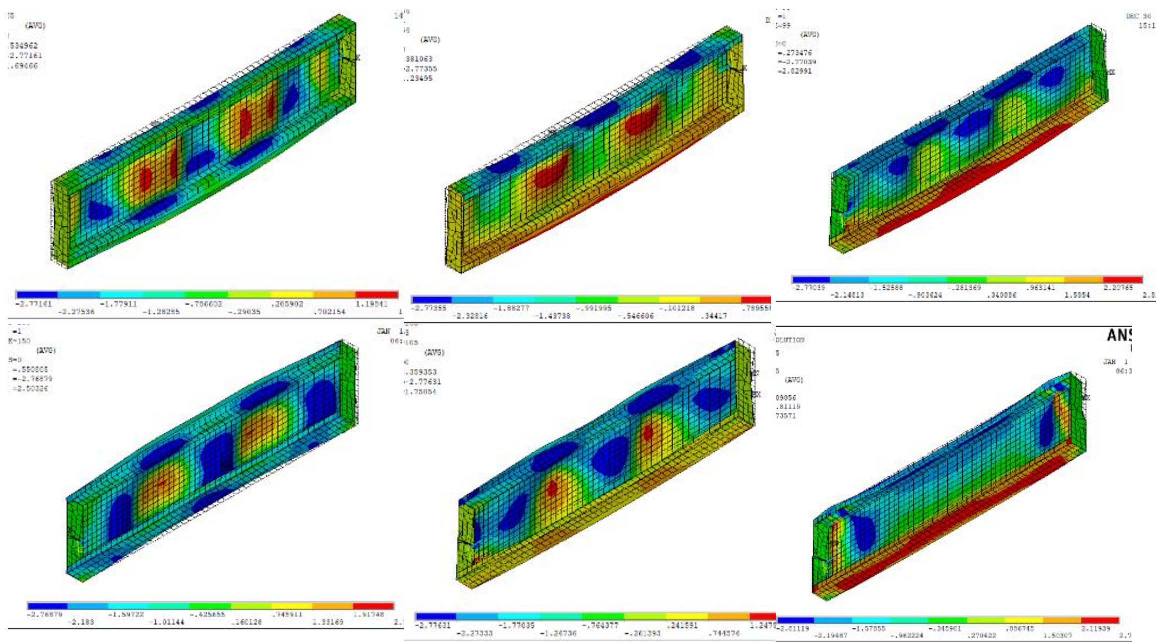

Pure axial loads | Combined axial loads and Major axis bending moments | Pure Major bending moments

Figure 5: Failure modes and Von Misses stresses distribution, Channel section, L/r_y = 50

It is conspicuous that, for short members having lipped channel sections, the ultimate strength is significantly affected by the section thickness. It is reduced when the section become more thin. The percent reduction is obvious when the member is loaded by higher values of axial forces than bending moments. As the section thickness decreased from 2.5mm to 1.5mm, the capacity reduced by 25% when it is loaded only by axial loads. This percent become 20% if it is loaded by combination of axial loads and bending moments (axial loads equal 60% of the squash loads), and relatively vanished when it is loaded only by bending moments. However, this is not clear for long members, L/r_y = 150, having channel sections, where there is no big change in the strength with changing the section thickness. On the other hand, short and long members having sigma sections, there are remarkable drop in the strength (about 30%) by decreasing the thickness from 25.mm to 1.5mm when the member is loaded by higher values of axial loads.

Although the interaction relation is linear for long members having channel sections, it is concave upward for the other cases.

t = 1.5mm

t = 2.5mm

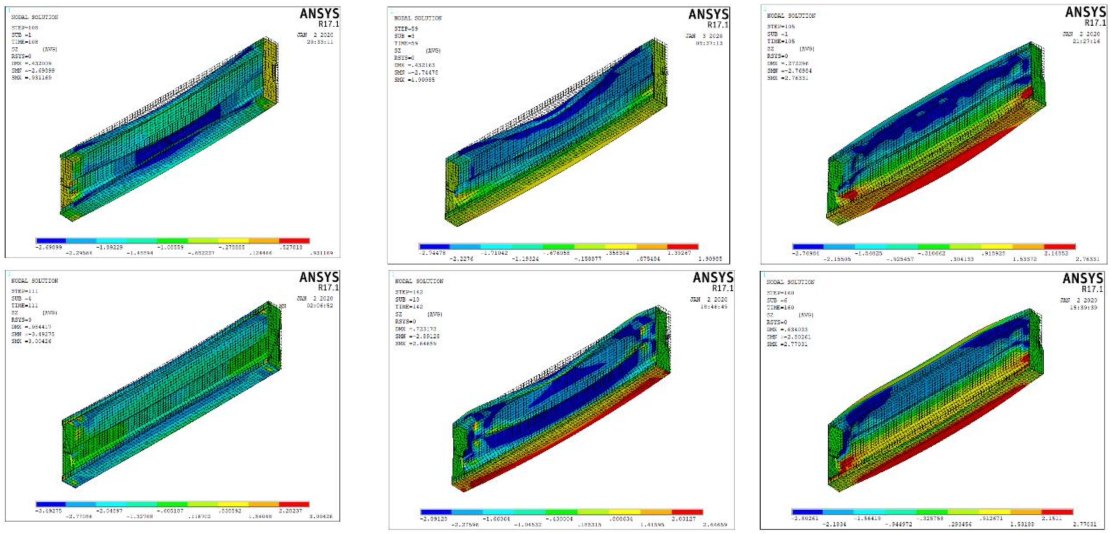

Pure axial loads | Combined axial loads and Major axis bending moments | Pure Major axis bending moments

Figure 6: Failure modes and Von Misses stresses distribution, Sigma sections, $L/r_y = 50$

Close observation to the failure shapes revel that, in short lipped channel members, when the axial force has big contribution failure is triggered by local buckling waves in the web which has significant post buckling reserve capacity. On the other hand when the bending moment ratios goes up the mode of failure turns into distortional buckling in the flanges, which has less post buckling reserve capacity. However, In sigma section due to the stiffening of the web, local buckling waves are not observed, and failure controlled by distortional buckling in the flanges. For long member slenderness ratios, L/r_y = 150, the mode of failure is mainly the overall buckling mode. Figures 5 and Fig. 6 show the failure shapes of short lipped channel and sigma section members; respectively, whereas that of long members are depicted in Fig. 7.

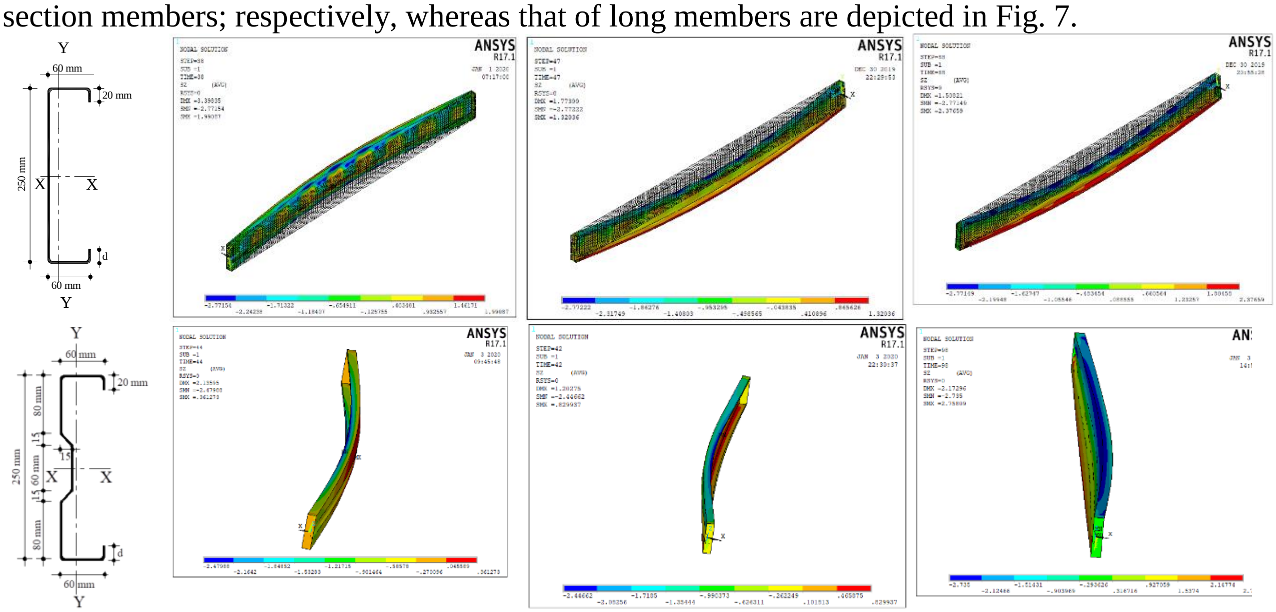

Pure axial loads | Combined axial loads and bending moments | Pure bending moments

Figure 7 : Failure modes and Von Mises stresses distribution Channel and Sigma sections, t = 1.5mm, L/r_y = 150

4-2 Axial compressive force and minor axis bending moments

In this section, the combined strength of the lipped channel and sigma section subjected to minor axis bending moments, Myu, and axial compressive force, Pu, has been determined using the developed nonlinear finite element model. The ratio of P_u/P_y is plotted against M_{yu}/M_{yy} in Fig.8. Where, M_{yy} represents the first yield minor axis bending moment, and it is determined as the product of the yield stresses by the minor axis full elastic section modulus. The positive direction of M_{yu}/M_{yy} represent the case when compression acting on the web, while the cases when compression acting on the lip are plotted in the negative direction.

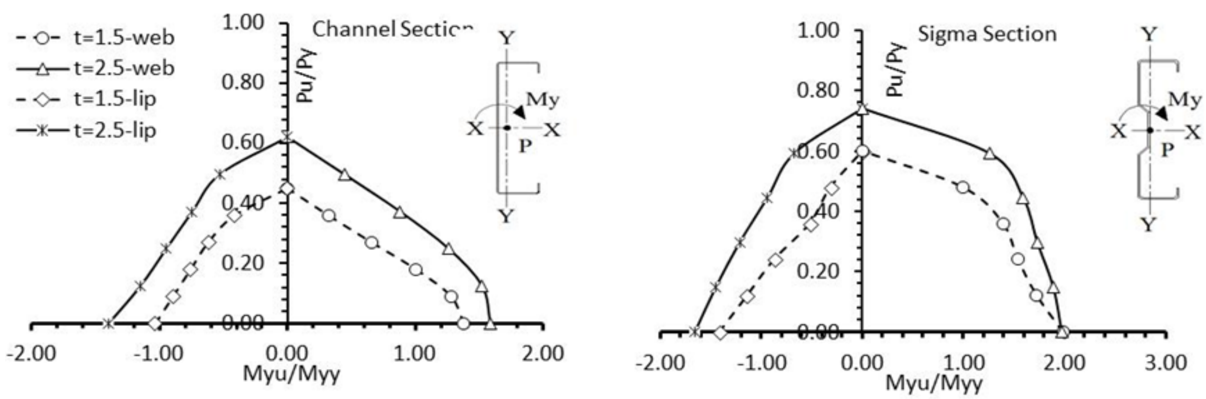

a) Channel sections b) Sigma sections

Figure. 8: Relation between P_u/P_y and M_{yu}/M_{yy}, $L/r_y = 50$

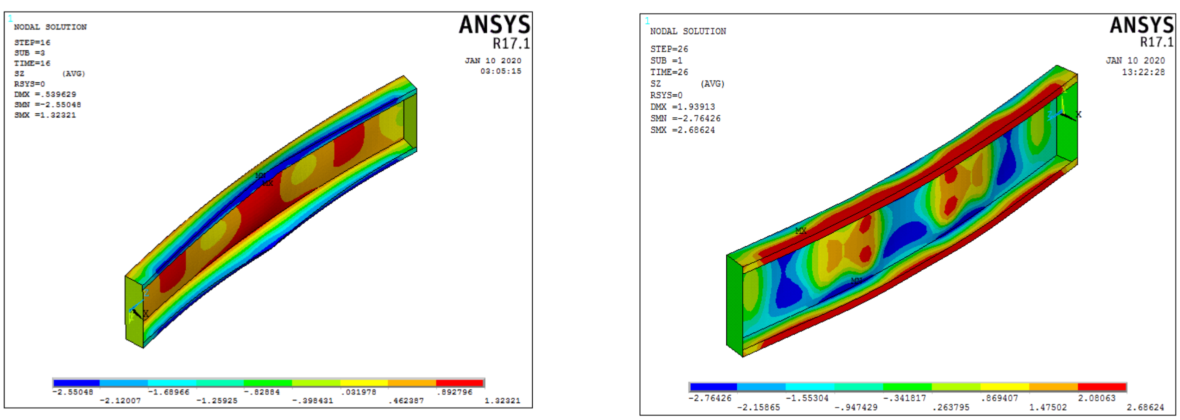

a) Compression on the lip b) Compression on the web

Figure 9 : Failure modes and Von Misses stress distribution, Channel sections, t = 1.5mm, $L/r_y = 50$ (M_{yu} only)

Similarly, these figures show that, the member strength go down by decreasing the section thickness. This reduction becomes more significant with increasing the axial load ratios, P_u/P_y. The average percentage reduction in the strength are 25% and 15 % when $P_u/P_y = 0.6$, and 0.2;

respectively. Moreover, there are substantial inelastic reserve capacity when the section loaded only in pure minor axis bending moments, M_{yu}, as the ultimate pure minor axis bending moments, are higher than the first yield bending moment, M_{yy}. This additional strength is higher when the bending moments cause compression on the web. For channel sections with thickness, t= 2.5mm, the M_{yu}/M_{yy} = 1.6 and 1.4, when the moment causing compression on the web and lip; respectively, and these ratios M_{yu}/M_{yy}, reduced to 1.35 and 1.05 when the section thickness, t=1.5mm.

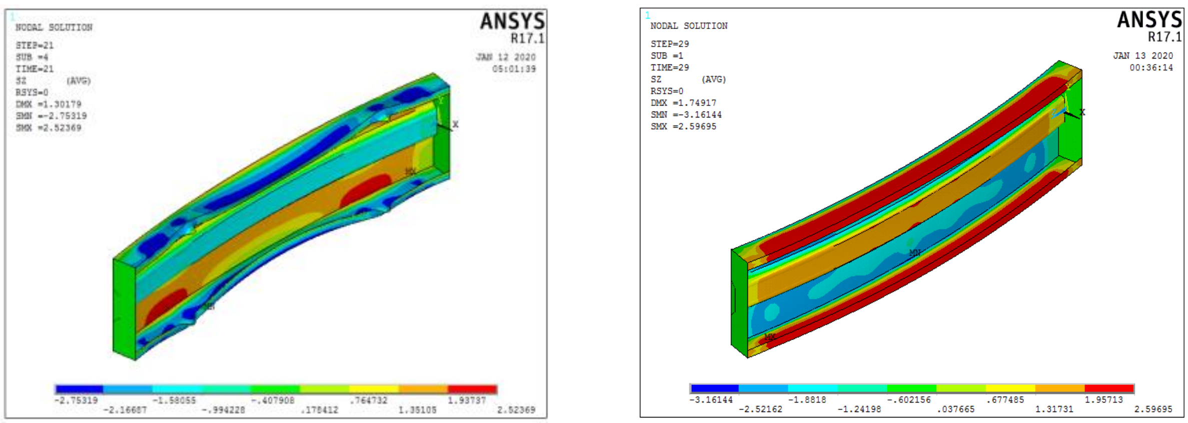

a) Compression on lip

b) Compression on web

Figure 10 : Failure modes and Von Misses stress distribution, Sigma sections, t = 1.5mm, L/r_y = 50 (M_{yu} only)

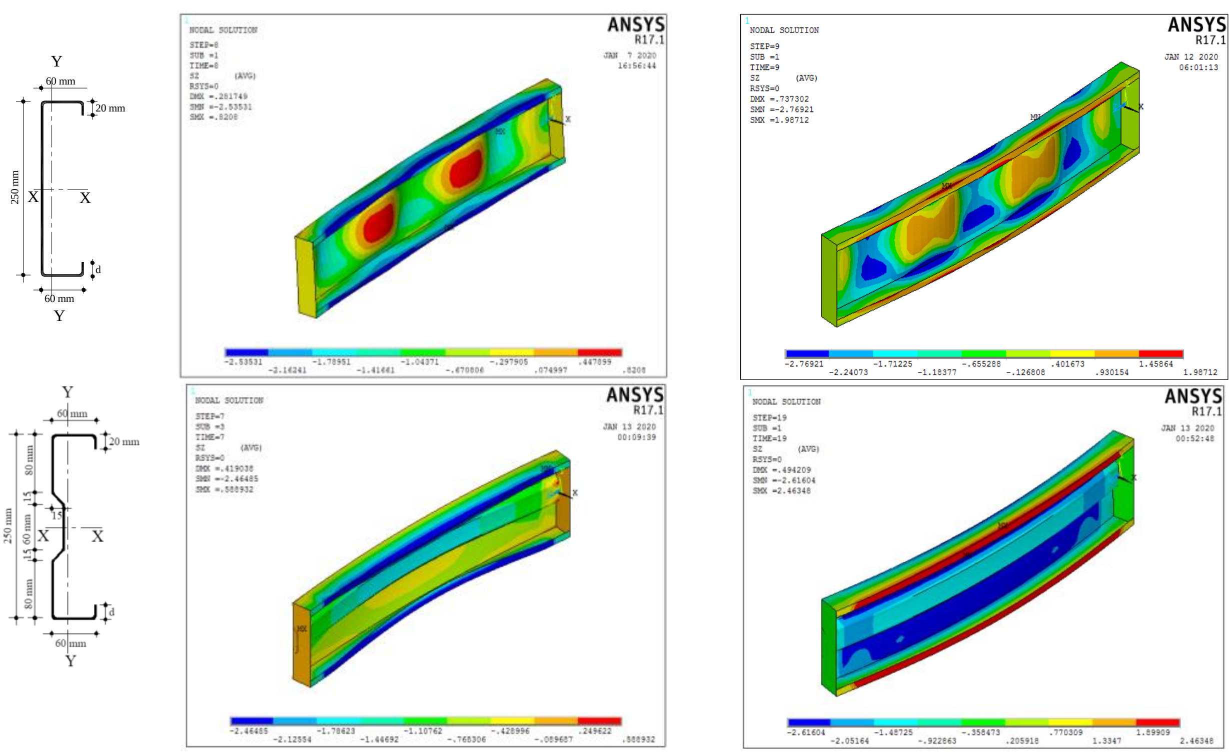

c) Compression on lip

d) Compression on web

Figure 11 : Failure modes and Von Misses stress distribution, Channel and Sigma sections,
t = 1.5mm, L/r_y = 50 (0.6P+My)

The observed failure modes are controlled by distortional buckling in the flanges when the member loaded in pure minor axis bending moments causing compression on the flange, however, in channel sections, series of local buckling waves are formed in the web when it become in compression, this is not observed in sigma sections. In both cases, the failure modes are associated by spread of yielding along the member on the compression and tension sides. Failure modes are depicted in Figs. 9, 10, and 11 for the case of pure minor axis bending moments, and combined axial plus minor axis bending moments; respectively.

5 - Comparison with standard codes

For sake of comparison, The obtained ultimate combined axial loads and bending moments are correlated with that predicted by AISI-2017. In this comparison, the ultimate pure axial force, P_{uo} as well as ultimate pure bending moments, M_{xu} & M_{yu}, are calculated using the *DSM* approach. In this approch, the axial as well as the flexural strength will be the minimum of the local, distortional, and the overall buckling strength. Moreover, the new *DSM*, Shahabeddin Torabian, et. al (2014), that incorporate stability under actual applied P-M_x-M_y action are employed. In the new *DSM*, the actual stresses due to the combined action of axial force and bending moments are used to get the corresponding buckling loads (local, distortional, global). Note that, calculation of the elastic critical local, distortional, and global buckling stresses have been determined using CUFSM V4.06 computer program. If unique minima does not exist, the *cFSM* , Adany, S., Schafer, B.W. (2006) , is used to get the critical half wave length at which the relevant pure mode occurs, Fig. 12 illustrate the signature buckling curve for different cases of loading. Note, the partial safety factors, γ_{M1}&ϕ_c, are not included when calculating the design loads.

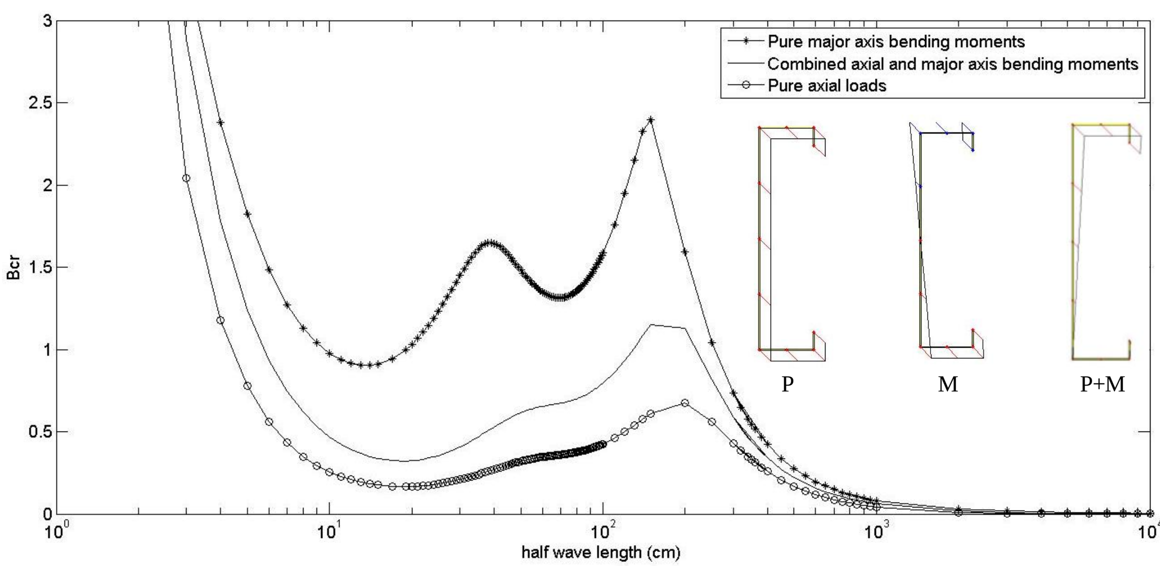

Figure 12: Signature buckling curve for channel section, t=1.5mm

$$\frac{P}{P_c} + \frac{a_x M_x}{M_{xc}} + \frac{a_y M_y}{M_{yc}} \leq 1 \tag{1}$$

where:

P	=	Design axial force
M_x	=	Design bending moments about major axis bending (x-axis)
M_y	=	Design bending moments about minor axis bending (y-axis)
P_u	=	Allowable pure axial force according to the specified code
M_{xu}	=	Allowable pure bending moment about major axis according to the specified code
M_{yu}	=	Allowable pure bending moment about minor axis according to the specified code
a_x, a_y	=	Amplification factors for bending moments according to the specified code

The ultimate axial forces are normalized with respect to the ultimate axial forces when there are no bending moments, P_{uo}. Also, the ultimate bending moments are normalized with respect to the ultimate bending moments when there are no axial forces, M_{uo}. The relation between, P/P_{uo} and M_u/M_{uo} are shown in Fig. 13 for the combined axial and minor axis bending, whereas, Fig.14 illustrates the results for combined axial and major axis bending. On the same figure the linear interaction equation, Eq. 1. that is adopted in AISI-2017 is presented, along with that predicted by new DSM.

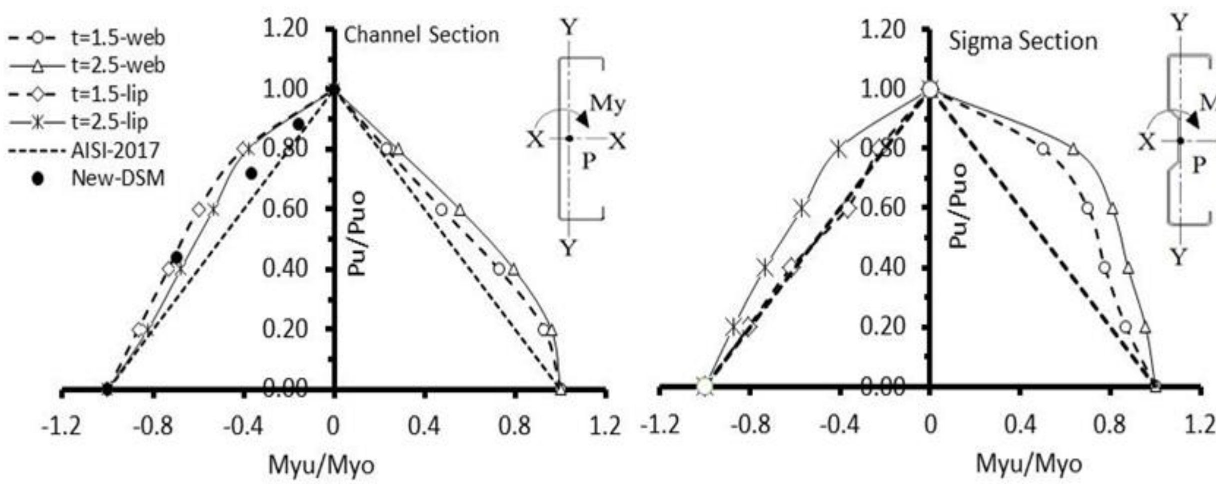

a) Channel Section b) Sigma Section

Figure 13 : P_u/P_{uo} versus M_{yu}/M_{yuo} (axial force + minor axis bending moments)

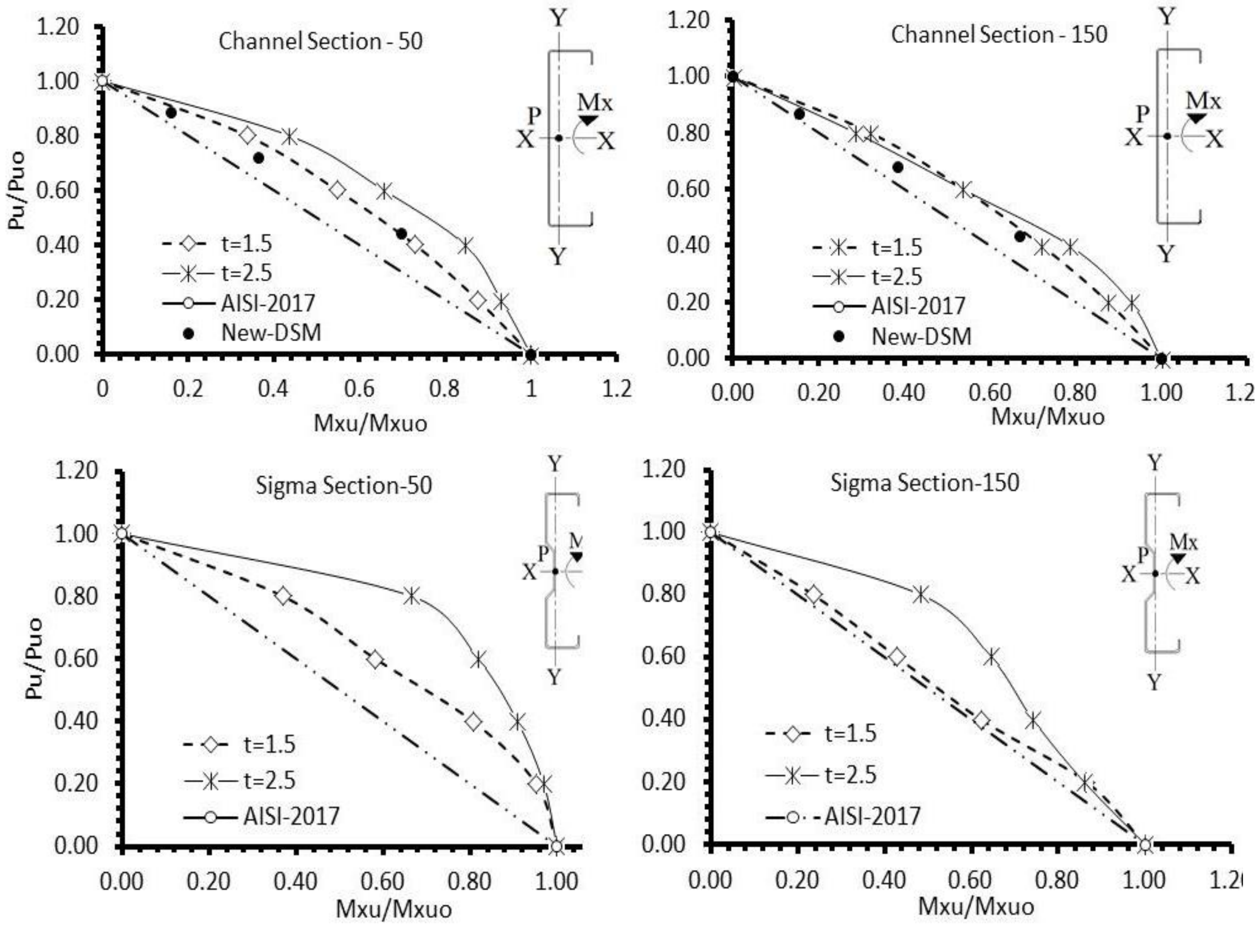

a) $L/r_y = 50$ b) $L/r_y = 50$

Figure 14 : P_u/P_{uo} versus M_{xu}/M_{xuo} (axial force + major axis bending moments)

Comparison revels that, the linear interaction relation that is adopted in AISI-2017 is conservatively predicate the combined axial and bending strength of cold formed sections, since most of the interaction relations are nonlinear. The obtained numerical strength could be 30% higher than that predicted by AISI-2017 especially when the member loaded byhigh portions of axial loads. Further, findings of the newly DSM are matched with that achieved by finite element results.

6. Conclusions

In this study, a finite element model was established to investigate the structural behavior of beam columns consists of single channel as well as sigma sections, and also to evaluate the appropriateness of the current design codes. Parametric study has been done including section thicknesses as well as the overall member slenderness ratios. Results revel that the numerical and experimental ultimate loads as well as failure modes are comparable. Moreover, the sectional geometric imperfection modes as well as residual stresses pattern have no remarkable effect on the ultimate capacity of the columns. Further, for short members the capacity greatly affected by the section thickness when it is loaded mainly by pure axial load as the failure mode is initiated by local buckling waves in the web. However, if the ratios of the applied moments increase the failure shape turned into distortional buckling in the flanges which have less post buckling capacity. To add on, there are significant inelastic reserve capacity when the section loaded only in pure minor axis bending moments. This additional strength is higher when the minor bending moments cause compression on the web. Finally, comparison with design codes reflects that, the combined axial and bending strengths determined by the linear interaction equation in AISI-2017 are conservative, since in most cases the interaction relations are not linear, however, it is concave upwards. Besides, results of the newly *DSM* are matched with that achieved by the developed finite element model.

References

AISI-S100 (2017). "North American Specification for the design of cold-formed steel structural members." *Washington (DC, USA): American Iron and Steel Institute*.

ANSYS, (2012) , Desalvo, G.J., and Gorman, R.W., *Swanson Analysis Systems*, Houston, PA.

A.H. Salem, M. El Aghoury, F.F. El Dib, and M.T. Hanna,(2007). "Strength of Bi-Axially Loaded Slender I-Section Beam-Columns". *Can. J. Civ. Eng.*, 34, 219-227.

Adany, S., Schafer, B.W., (2006) "Buckling mode decomposition of single-branched open cross-section members via finite strip method: Application and examples", *Thin-Walled Structures*, Vol. 44, pp. 585-600.

CUFSM v4.06 "Elastic Buckling Analysis of Thin-Walled Members by Finite Strip Analysis, http://www.ce.jhu.edu/bschafer/cufsm.

D.J Klingshirn, E. A. Sumner, and N. A. Rahman. (2010) "Experimental Investigation of Optimized Cold-Formed Steel Compression Member" *Twentieth International conference on cold-formed steel structures, St. Louse, Missouri, U.S.A.*, November 3&4.

El Aghoury M. A., Hanna M. T., Amoush E. A. (2017) "Experimental and theoretical investigation of cold-formed single lipped sigma column" *Thin-Walled Structures*; 111:80–92.

Hong-Guang Luo, Yao-Jie Guo and Shi-Cheng Ma. (2011) "Distortional buckling of thin-walled inclined lipped channel beams bending about the minor axis". *Journal of Constructional Steel Research. 67*, 1884–1889.

Long-yuan Li and Jian-kang Chen. (2008) "An analytical model for analysing distortional buckling of cold-formed steel section". *Thin-Walled Structures. 46*, 1430– 1436.

N. Silvestre, D. Camotim. (2004) "Distortional buckling formulae for cold-formed steel C- and Z-section members. Part I-Derivation". *Thin-Walled Structures 42*, 1567–1597

N. Silvestre, D. Camotim. (2004) "Distortional buckling formulae for cold-formed steel C- and Z-section members. Part II-Validation and application". *Thin-Walled Structures 42*, 1599–1629.

P. Nandini, V. Kalyanaraman. (2010). "Strength of cold-formed lipped channel beams under interaction of local, distortional and lateral torsional buckling" *Thin-Walled Structures 48*, 872–877.

Schafer B. W. (2008) "Computational Modeling of Cold-Formed Steel" *Fifth International Conference on Coupled Instabilities in Metal Structures*, Sydney, Australia, 23-25.

Shahabeddin Torabian, Baofeng Zheng, and Benjamin W. Schafer. (2014) "Development of a new beam-column design method for cold formed steel lipped channel members " *22nd International conference on cold-formed steel structures, St. Louse, Missouri, U.S.A.*

Shahabeddin Torabian, David C. Fratamico, and Benjamin W. Schafer. (2015) "Experiments on cold-formed steel Zee-shaped stub beam-columns " *Annual stability conference, structure stability research council, Nashville, Tennesse, March 24-27.*

Zeinoddini V. M., Schafer B. W. (2012). "Simulation of geometric imperfections in cold-formed steel members using spectral representation approach" *Thin-Walled Structures 60*, 105–117